EXPERIMENT PROGRAM OF SHAKE TABLE TEST ON A PRECAST FRAME MADE OF RECYCLED AGGREGATE CONCRETE

PHAM THI LOAN
Hai Phong University, Vietnam – Email: loanpt80@dhhp.edu.vn

PHAN VAN HUE
Mien Trung University of Civil Engineering, Vietnam – Email: phanvanhue@muce.edu.vn

(Received: September 09, 2016; Revised: October 25, 2016; Accepted: December 06, 2016)

ABSTRACT

A precast frame model made of Recycled Aggregate Concrete (RAC) been constructed with precast beams, columns and Cast-In-Place (CIP) joints. Then a shaking table test was carried out with three types of earthquake ground motions, namely Wenchuan, El Centro and artificial Shanghai waves. Based on the shaking test, the test program is presented and analyzed. The paper focuses on the shaking test program, including materials, similitude law and scaled model, instruments, seismic waves and loading program. Consequently, a comprehensive understanding on the process of shake table test is revealed thanks to the results of an investigation on a precast frame structure made of recycled aggregate concrete.

Keywords: frame structure; precast; recycled aggregate concrete (RAC); shake table test; peak ground acceleration; similitude law.

1. Introduction

Construction and demolition (C&D) waste constitutes a major portion of total solid waste production in the world. In addition, natural disasters such as earthquakes also significantly contribute to the abundance of the waste concrete. Therefore, the most effective way to reduce the waste problem in construction is agreed in implementing reuse, recycling and reduced the use of a construction material in construction activities. The reason is that, recycling concrete materials has two main advantages - it conserves the use of natural aggregate and the associated environmental costs of exploitation and transportation, and it preserves the use of landfill for materials which cannot be recycled.

Since the study on fundamental behaviors of Recycled Aggregate Concrete (RAC) is well-documented in the current literature, its mechanical properties are accordingly explored (Bhikshma & Kishore, 2010; Fonseca, 2011; Xiao, J.Z, Li, Fan, & Huang, 2012). For instance, the compressive, tensile and shear strengths of RAC are generally lower than those of Natural Aggregate Concrete (NAC); the modulus of elasticity for RAC generally reduces as the content of Recycled Coarse Aggregate (RCA) increases; the RCA replacement percentage has nearly no influence on the bond strength between RAC and deformed rebars. In addition, the properties of RAC are greatly influenced by of the mix proportion (Parekh & Modhera, 2011) and it is clearly known that mixing concrete will be controlled much better in factory conditions. Therefore, the authors suggest that RAC components can be produced in precast factories in order to take inherent advantages of precast elements and ensure the quality of construction (Xiao, J.Z., Pham, Wang, & Gao, 2014). Prefabrication of building elements in a factory condition brings with its certain inherent advantages over purely site-based construction. For instance, speed, quality and efficiency, they are all cited as specific attributes of precast construction.

Added to these, studies on the structural performance of RAC have also been investigated not only on elements but also on structures subjected to both static and dynamic loads. The studies on beams (Mahdi, Adam, Jeffery, & Kamal, 2014; Xiao, J.Z. et al., 2014), columns (Tam, Wang, Tao, & Tao, 2014; Xiao, J. Z., Huang, & Shen, 2012) and slabs (J. Z. Xiao, Sun, & Jiang, 2015) have contributed to understanding failure patterns, flexure, shear and compression behavior of RAC elements. Besides, beam-column joints and plane frames have also been tested under cyclic loading (Corinaldesi & Letelier, V., 2011; J. Z. Xiao, Tawana, & Wang, 2010). Noticeably, shaking table tests on RAC structures were investigated by the authors recently (J. Z. Xiao, Wang, Li, & Tawana, 2012; J. Xiao, Pham, & Ding, 2015). The results proved that RAC structures show a good seismic performance. Therefore, the positive results from these serial studies indicate the possibilities of applying RAC in civil engineering structures.

One important point should be kept in mind that the properties of RAC are influenced greatly by preparation condition of mix proportion. Therefore, it is strongly suggested that RAC should be prepared and mixed under a controlled environment such as in precast factories in order to ensure not only the quality of constructions but also take inherent advantages of precast structures. From the view of combination between RAC and precast, the precast RAC components are feasible to use and develop application of RAC in civil engineering as structural materials.

Precast concrete structures made of NAC are widely used in many countries, especially in the United States, New Zealand, and Japan where moderate-to-severe earthquakes often occur. Observing from some earthquake events recently, such as Kobe earthquake in Japan in 1995 and Christchurch earthquake in New Zealand in 2011, the on-site reports and observations of damage to reinforced concrete buildings indicated that both cast-in-place and precast concrete frame structures performed similarly under earthquake attack by the means of capacity design and proper connection detailing of the precast concrete elements (Elwood, Pampanin, & Kam, 2012).

The seismic performance of precast concrete structure depends on the ductility capacity of the connectors jointing each precast component, especially at critical joints such as the beam-to-column connections. Therefore, the development of the seismic connections is essential in the precast construction. The detail and location of precast concrete connections have been the subjects of numerous experimental and analytical investigations (Alcocer, Carranza, Navarrete, & Martinez, 2002; Ericson, 1994; J. Z. Xiao et al., 2010). Most of the precast concrete constructions adopt connection details emulated Cast-In-Place (CIP) concrete structures so that they should have equivalent seismic performance as monolithic concrete members. For instance, the failure patterns, strengths and drift ratios as well as ductility were satisfied in comparison with monolithic specimens in those researches.

Therefore, a 6-story precast RAC building has been constructed using CIP concrete made of recycled coarse aggregate (RCA) to complete the joints between precast components in order to investigate earthquake response by the shaking table test.

2. Shaking table test

2.1. General

The tested model was one-fourth scale model of a 2-bay, 2-span, and 6-story precast frame structure made of RAC. The test was conducted at the State Key Laboratory for Disaster Reduction in Civil Engineering at Tongji University. The main parameters of the shaking table are:

Table size: 4000-mm x 4000-mm x 800-mm

Vibration waveform: cyclic, random, earthquake

Maximum specimen weight: 250 kN

Operation frequency range: 0.1 to 50 Hz

Controlled degree of freedom: 6

Maximum acceleration: X up to 1.2g; Y up to 0.8g; Z up to 0.7g

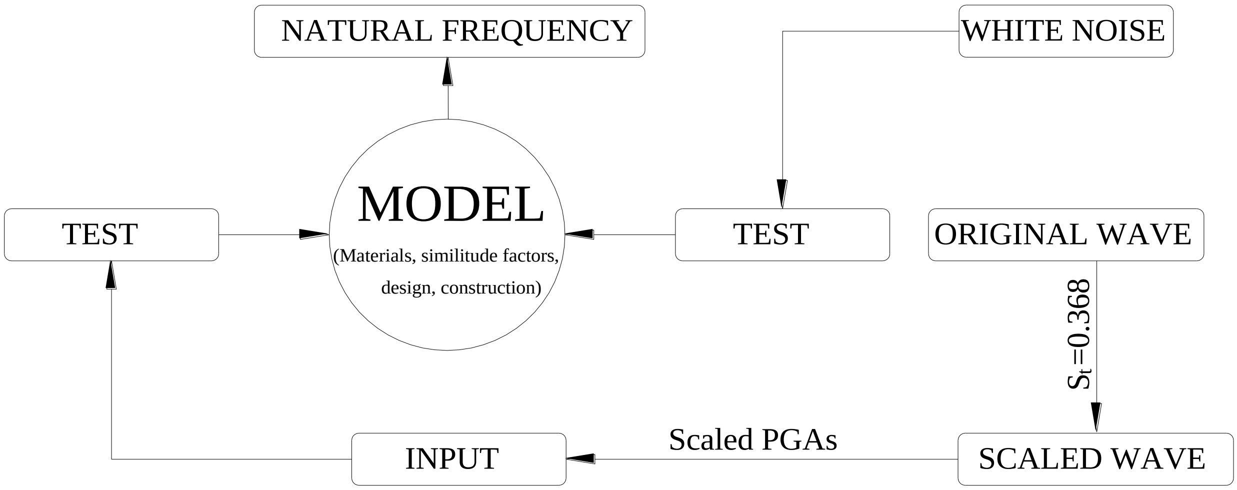

Figure 1. Process of shaking table test

2.2. Materials

Recycled coarse aggregates (RCA) were produced from aged concrete that has been demolished and most of the compressive strength for demolished concrete is ranged from 17.5MPa to 25MPa.

(a) Debris of concrete

(b) Produced aggregate

(c) Recycled coarse aggregate

Figure 2. Plan of RAC production

Recycled aggregates can be produced in plants similar to those used to crush and screen conventional natural aggregates. Large protruding pieces of reinforcing steel are first removed by hydraulic shears and torches. Then a jaw crusher is often selected for primary crushing because it can handle large pieces of concrete and residual reinforcement. Jaw crushers also fracture a smaller proportion natural aggregate in of the parent concrete aggregate. The residual reinforcement is removed by large electro-magnets. Impact crushers are preferred for secondary crushing as they produce a higher percentage of aggregate without adhered mortar. In general the shape of recycled aggregate is rounder and less flaky than natural aggregate. Due to the scale factor of the tested model, RCA was sieved in the range from 5-10 mm. The measured apparent density of the RCA was 2481 kg/m^3 and the water absorption was 8.21%.

The recycled concrete mixture of nominal strength grade C30 was proportioned with the recycled coarse aggregates (RCA) replacement percentage equal to 100% with slump value in the range 180−220 mm. The fine aggregate used was river sand. The applied coarse aggregate was recycled coarse aggregate with properties as described above. The mix proportions of the concrete were described in Table 1. Due to the high water absorption capacity of recycled concrete aggregates, the recycled concrete aggregates used were presoaked by additional water before mixing. The water amount used to presoak the recycled concrete aggregates was calculated according to the saturated surface-dried conditions.

Table 1

Mix proportions of recycled concrete

W/C(%)	S/A(%)	S(kg/m^3)	C(kg/m^3)	W(kg/m^3)	WA(kg/m^3)	SP(kg/m^3)
53	41	682	396	213	38.8	3.96

Note: C=cement content, S= sand content, S/A=fine aggregate (sand) to total aggregate percent, W= mixing water content, WA=additional water content, SP= super plasticizer content.

According to Chinese standard GB50010-2002 code (Chinese Standard Code GB50010-2010, 2002) and similarity relation of the frame model, fine iron wires were used to model rebars. Galvanized steel wires of 8# (diameter of 3.94 mm) and 10# (diameter of 3.32 mm) were adopted as the longitudinal reinforcement and 14# (diameter of 2.32 mm) for transversal reinforcement in this model.

The measured average mechanical properties of the fine iron wires related to the frame model are shown in Table 2.

Table 2

Mechanical properties for reinforcement

Specifications	Diameter(mm)	Yield strength (MPa)	Ultimate strength (MPa)	Elastic modulus (GPa)
8#	3.94	358	407	200
10#	3.32	306	388	200
14#	2.32	252	363	200

2.3. Similitude factors

Based on dimensional analysis-Buckingham's Pi theorem (Buckingham, E., 1914) and similitude requirements for dynamic loading, the variables that govern the behavior of vibrating structures reveals that in addition to length (L) and force (F), which we considered in static load situations, we must now include time (T) as one of the fundamental quantities before we proceed with dimensional analysis. Therefore, it is logical to choose S_L, S_E and S_a. The remaining scale factors are then calculated and given in Table 3. It is well-known that the shaking table test was conducted on the earth, so the gravity acceleration applied in the model and prototype are the same (Zhang, M., 1997). So the similarity coefficient of gravity acceleration equals 1.

Table 3
Similitude factors between the prototype and the test mode

Physical Property	Physical parameter	Formula	Relationship	Remark
Geometry parameters	Length	S_l	**0.25**	Control the dimension
	Displacement	$S_\delta = S_l$	0.25	
Material property	Elastic modulus	S_E	**1.00**	Control the material
	Stress	$S_\sigma = S_E$	1.00	
	Poisson's Ration	S_υ	1.00	
	Strain	$S_\varepsilon = S_\sigma / S_E$	1.00	
	Mass density	$S_\rho = S_\sigma / S_a S_l$	2.165	
	Mass	$S_m = S_E S_l^2 / S_a$	0.034	
Load	Area load	$S_p = S_\sigma$	1.00	
	Concentrated force	$S_F = S_E S_l^2$	0.063	
Dynamic performance	Period	$S_T = S_l^{1/2} / S_a^{1/2}$	0.368	
	Frequency	$S_f = S_l^{-1/2} / S_a^{-1/2}$	2.719	
	Velocity	$S_v = S_l^{1/2} . S_a^{1/2}$	0.680	
	Acceleration	S_a	**1.848**	Control the shaking table test
	Acceleration of gravity	S_g	1.00	

However, the model is practically impossible to build with such a mass density and the model was used same material in prototype. It means that, S_ρ was equal to 1 instead of the values obtained from similitude law. Therefore, additional mass to scaled model structure was required.

The mass of the model with the required density of material as calculated as follows:

$m_m^{re} = m_p . S_m^{re}$

$m = \rho . V$ and $V = l^3 \rightarrow S_m = S_\rho . S_V = S_\rho . S_l^3$

Hence,

$$m_m^{re} = m_p . S_\rho^{re} . S_l^3 \quad (1)$$

However, mass density of material provided is equal to 1, resulting in the mass of the model with provided density of material as:

$$m_m^{pro} = m_p . S_\rho^{pro} . S_l^3 = m_p . S_l^3 \quad (2)$$

Consequently, additional mass to scaled model was required:

$$\Delta m = m_m^{re} - m_m^{pro} = m_p . S_\rho^{re} . S_l^3 - m_p . S_l^3 = m_p . S_l^3 (S_\rho^{re} - 1)$$

$$S_\rho^{re} = \frac{S_\sigma}{S_a S_l} = \frac{1}{S_a S_l} \rightarrow \Delta m = m_p . S_l^3 (S_\rho^{re} - 1) = m_p \left(\frac{S_l^2}{S_a} - S_l^3 \right)$$

Since $S_g = 1$, the additional weight required added to the scaled model was:

$$\Delta W = W_m^{pro} . \frac{\frac{S_l^2}{S_a} - S_l^3}{S_l^3} \quad (3)$$

where, m_m^{re} *is the mass of the model with the required density of material;* m_m^{pro} *is the mass of the model with the provided density of material;* m_p *is the mass of the prototype structure;* W_m^{pro} *is the weight of the model with the provided density of material.*

As a result, weight of 4.914 tons is added to simulate the required density of material and weight of 3.835 tons was added to simulate dead and live load. Totally, weight of 8.925 tons is represented by the iron blocks and plates. The arrangement of the iron blocks and plates, which detail are shown in Table 4, are given in Figure 3. Finally, the total weight of model was estimated to be 17 tons including the base beams, which was less than the capacity limitation of the shaking table.

Table 4
Number of iron blocks and plates (piece)

Name	Dimension	Weight (kg)	Quantity (piece)		
			2nd to 6th	Roof	Total
Steel plate	400x20	20.0	32	28	188
Cube 3.5	100x100x50	3.5	247	223	1458
Cube 1.0	100x50x40	1.0	8	22	62

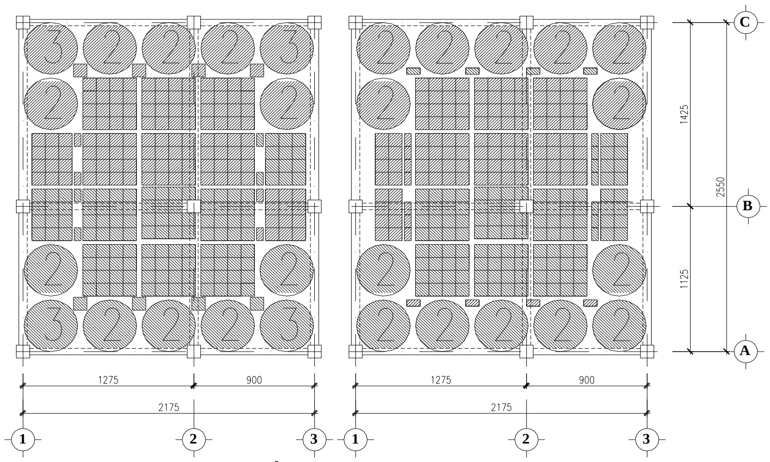

(a) 1st to 5th floor (b) Roof floor

Figure 3. Arrangement of steel plate and cube mass on floors

2.4. Fabrication and construction of the model

The process of producing the model included two stages: (1) fabricate beam and column elements in a factory and (2) construct the precast model in Lab. This section is to discuss that process in briefly.

The precast elements consisted of two types of components, one is 54 columns and one is 72 beams. These components were fabricated in the precast factory which was convenient for fabrication. The fabrication process was the same for two types of components. Firstly, reinforcing bars of both components were assembled into the reinforcing cages. Then the reinforcing cages were moved to the platforms that were used as the base forms, the wooden forms were coated with oil. All components were ready for casting. Ready-mix recycled concrete grade of C30 with the maximum size coarse aggregate of 10mm was used for all the specimens. The specimens casted were cured at ambient temperature for 28 days and transported to construction site of the lab as shown in Figure 4.

Figure 4. Precast elements on site

The in-situ foundation will provide a fixed base connection to the precast column, which is particularly useful in low rise precast industrial units where the cantilever action of the column provides the lateral stability for the building. The columns were embedded into the footing beam by a distance of at least 1.5 times the maximum column foot dimension The footing beam was then filled with in-situ concrete to fix the foot columns.

Figure 5. Detailing joint

Single story columns were erected at each floor level and the beams seated on the head of columns by beam rear for ease of construction. The continuity of longitudinal reinforcement through the beam-column joint was designed to ensure rigid beam-column connections as shown in Figure 5. With this method of precast construction, the model was erected one floor at a time with beams placed at the head of columns at one level before the upper level columns were erected and connected by welding bars. Then two layers of slab reinforcement were fixed in the forms, and RAC was poured for the joints and slabs.

The whole process of construction was completed after the top floor of the model was casted as presented in Figure 6(a). The model was cured in the laboratory at an ambient temperature for 28 days. To prepare for shaking table tests, the model was then moved and fixed on the shake table as shown in Figure 6 (b) and (c), respectively.

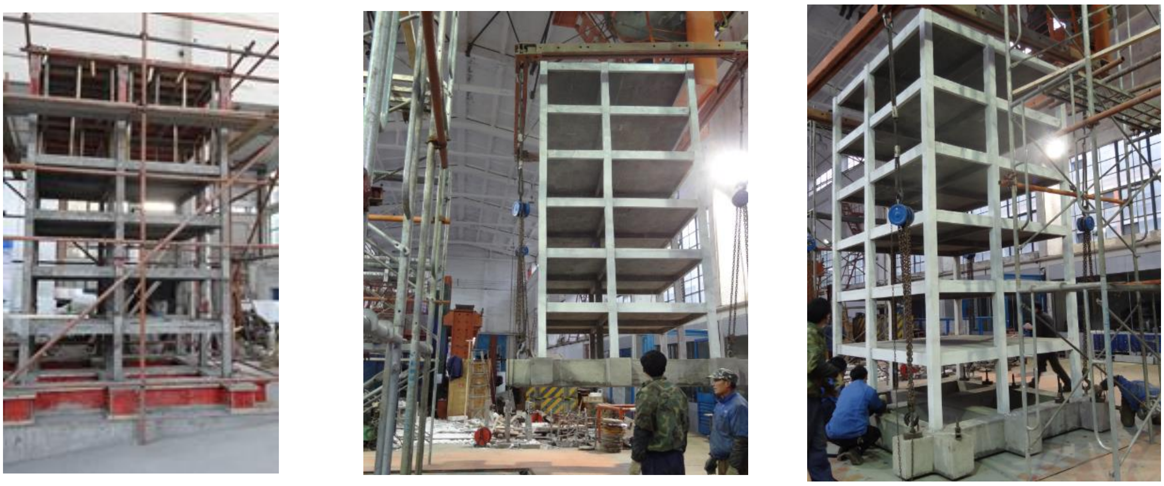

(a) Completed model (b) Moved model (c) Fixed model

Figure 6. Curing, moving and fixing model

2.5. Instruments

In order to monitor the global responses of the model structure during tests as well as the local state including crack developing, plastic hinge development of members, etc., a variety of instrumentation were installed on the model structure before shaking table tests. The accelerations and displacements were measured by accelerometers and displacement gauges, respectively.

A total of 28 accelerometers and 14 LVDTs were arranged throughout the test structure. All the accelerometers were set for recording the horizontal accelerations including 2 on the base beams, 4 on each floor from 1st to 5th and 6 on roof floor. All the displacement gauges were arranged to record the horizontal including 2 on each floor and 4 on the roof floor. The positions of total 28 accelerometers and 14 displacement transducers are clearly observed by 3-D photo as illustrated in Figure 7. The accelerometers and displacement transducers were embedded on the model as shown in Figure 8.

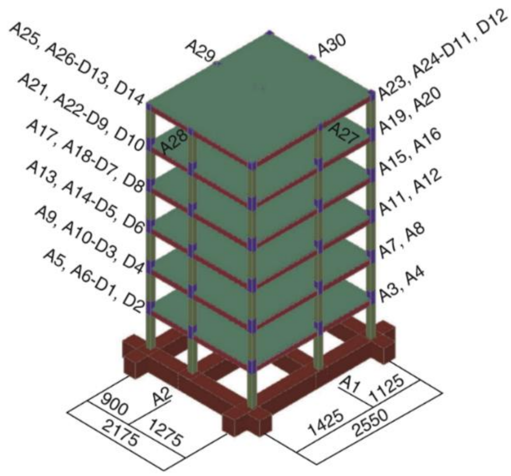

Figure 7. Arrangement of accelerometers and displacement LVDTs

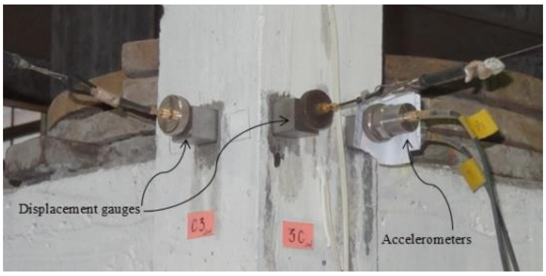

Figure 8. Accelerometers and LVDTs embedded on the model

2.6. Shaking table test

According to Code for seismic design of buildings GB 50011-2008 (Chinese Standard GB 50011-2010, 2008) , Wenchuan seismic wave (WCW, 2008, N-S) should be considered for Type-II site soil. According to the spectral density properties of Type-II site soil, El Centro wave (ELW, 1940, N-S), Shanghai artificial wave (SHW) are selected and described in the following. The time history of three seismic waves are shown in Figure 9.

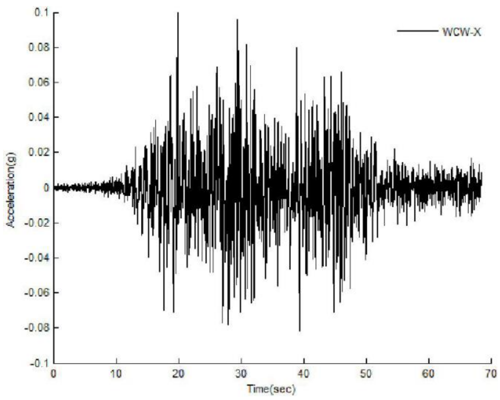

(a) WCW wave

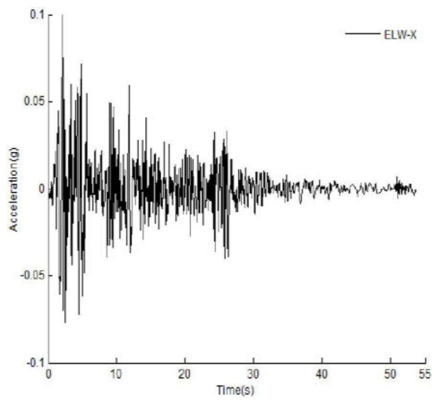

(b) ELW wave

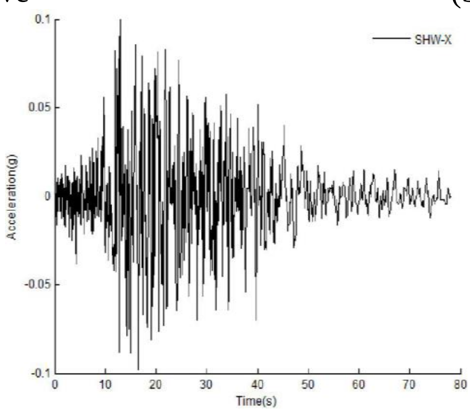

(c) SHW wave

Figure 9. Time history of three waves

The test program consists of eight phases, that is, tests for peak ground acceleration (PGA) of 0.066g, 0.13g (frequently occurring earthquake of intensity 8), 0.185g, 0.264g, 0.370g (basic occurring earthquake of intensity 8), 0.415g, 0.55g, 0.75g (rarely occurring earthquake of intensity 8 were set to evaluate the overall capacity and investigate the dynamic response of the recycled aggregate concrete frame structure. According to the similitude factors in Table 3.4, time scale 0.368 means that frequency scale is 2.719. The sequence of inputs was WCW, ELW and SHW in the test process. After different series of ground acceleration were input, white noise was scanned to determine the natural frequencies and the damping ratios of the model structure. And in this case, the peak value acceleration (PGA) of the white-noise input was designed to 0.05g in order to keep the model in the linear elastic deformation. The detail of loadings is listed in Table 5. The Table 5 indicates that the PGAs of the white-noise were smaller than 0.05g which met the purpose of design. The input PGAs of ELW show the best match with design values by the difference of around 5%. The differences of PGAs between inputs and designed values of WCW and SHW are mostly over 5%, especially in case of PGA of 0.185g for WCW and PGA of 0.37g for SHW, the both difference is 24.86%. The time history of inputs and outputs of shake-table recorded from any load cases were the same which are illustrated in Figure 10 as an example.

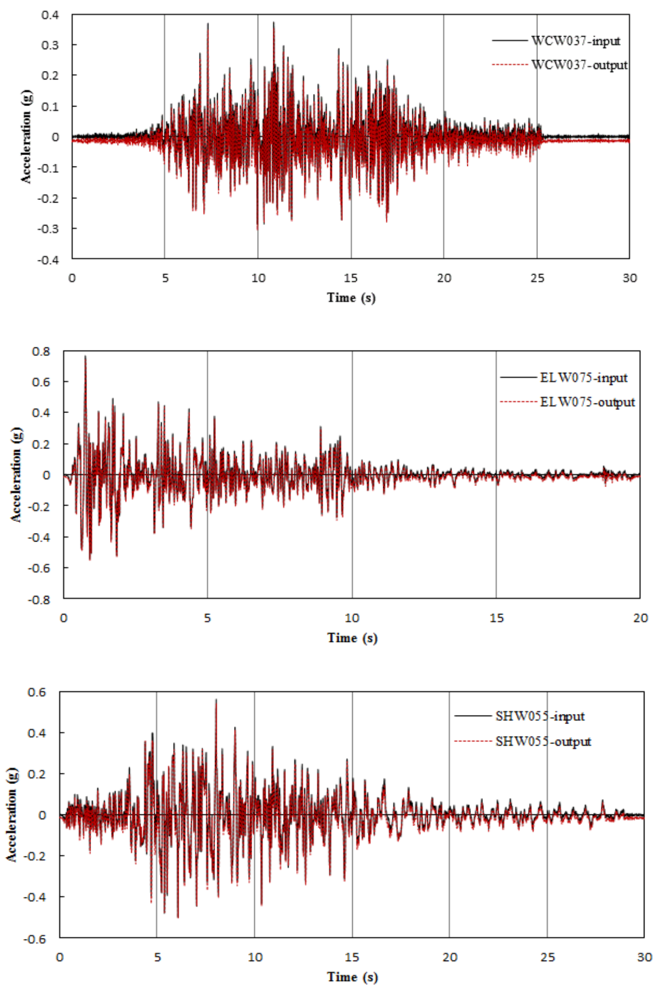

Figure 10. The time history of inputs and outputs motions.

Table 5
Loading Program

No.	Input	PGA (g)					
		Direction X			Direction Y		
		Designed	Measured	Variation (%)	Designed	Measured	Variation(%)
1	White noise	0.05	0.032	-36.00	0.05	0.0364	-27.2
2	WCW	0.066	0.0753	14.09	-		-
3	ELW	0.066	0.0668	1.21	-		-
4	SHW	0.066	0.0677	2.58	-		-
5	White noise	0.05	0.0368	-26.40	0.05	0.0378	-24.4
6	WCW	0.13	0.1395	7.31	-		-
7	ELW	0.13	0.135	3.85	-		-
8	SHW	0.13	0.1456	12.00	-		-
9	White noise	0.05	0.037	-26.00	0.05	0.0437	-12.6
9a	White noise	0.05	0.0359	-28.20	0.05	0.044	-12
10	WCW	0.185	0.231	24.86	-		-
11	ELW	0.185	0.197	6.49	-		-
12	SHW	0.185	0.175	-5.41	-		-
13	White noise	0.05	0.036	-28.00	0.05	0.046	-8
14	WCW	0.264	0.273	3.41	-		-
15	ELW	0.264	0.261	-1.14	-		-
16	SHW	0.264	0.269	1.89	-		-
17	White noise	0.05	0.035	-30.00	0.05	0.04	-20
18	WCW	0.37	0.374	1.08	-		-
19	ELW	0.37	0.349	-5.68	-		-
20	SHW	0.37	0.278	-24.86	-		-
20a	SHW	0.415	0.438	5.54	-		-
21	White noise	0.05	0.036	-28.00	0.05	0.046	-8
22	WCW	0.415	0.443	6.75	-		-
23	ELW	0.415	0.44	6.02	-		-
25	White noise	0.05	0.0344	-31.20	0.05	0.044	-12
26	WCW	0.55	0.595	8.18	-		-
27	ELW	0.55	0.548	-0.36	-		-
28	SHW	0.55	0.561	2.00	-		-
29	White noise	0.05	0.035	-30.00	0.05	0.042	-16
30	WCW	0.75	0.744	-0.80	-		-
31	ELW	0.75	0.766	2.13	-		-
32	White noise	0.05	0.036	-28.00	0.05	0.041	-18
33	SHW	0.75	0.679	-9.47	-		-
34	White noise	0.05	0.036	-28.00	0.05	0.044	-12

3. Conclusions

Based on analysis on the procedure of the 6-story precast frame made of recycled aggregate concrete, some conclusions and suggestions are presented in the following:

1. Investigations and development of applying RAC as a structural material in civil engineering have been widely.

2. Shaking table test plays an important method in order to perform seismic behaviors of structures subjected to earthquake loads.

3. Shaking table test program was presented and analyzed in detail. Among the main contents including materials, similitude

factors, designing the model, fabrication and erection, equipment, seismic waves and loadings, similitude factors and loading sequences were considered the most important and significant issues of a shaking table test on a scaled model.

4. The loading process was gradually increased which is not coincided with the real earthquake load affected to structures. However, this process has been employed in laboratories■

References

Alcocer, S. M., Carranza, R., Navarrete, D. P., & Martinez, R. (2002). Seismic Tests of Beam-to-Column Connections in a Precast Concrete Frame. *PCI Journal*, *47*(3), 70–89.

Bhikshma, V., & Kishore, R. (2010). Development of stress-strain curves for recycled aggregate concrete. *Asian Journal Civil Engineering (Building and Housing)*, *11*(2), 253–261.

Buckingham, E. (1914). On physically similar system. *Physical Review*, *4*(4), 345–376.

Chinese Standard Code GB50010-2010. Code for Design of Concrete Structures (2002).

Chinese Standard GB 50011-2010. Code for Seismic Design of Buildings (2008).

Corinaldesi, V., & Letelier, V. (2011). Behaviour of beam–column joints made of recycled-aggregate concrete under cyclic loading. *Construction and Building Materials*, *25*, 1877–1882.

Elwood, K. J., Pampanin, S., & Kam, W. Y. (2012). 22 February 2011 Christchurch Earthquake and Implications for Design of Concrete Structures. In *International Symposium on Engineering Lessons Learned from the 2011 Great East Japan Earthquake* (pp. 1157–1168). Tokyo, Japan.

Ericson, A. C. (1994). Emulation Design of Precast Concrete. *The Construction Specifier*, *47*(10), 96–103.

Fonseca, N. (2011). The influence of curing conditions on the mechanical performance of concrete made with recycled concrete waste. *Cement & Concrete Composites*, *33*, 637–643.

Mahdi, A., Adam, S., Jeffery, S. V., & Kamal, H. K. (2014). An experimental study on shear strength of reinforced concrete beams with 100% recycled concrete aggregate. *Construction and Building Materials*, *53*, 612–620.

Parekh, D. N., & Modhera, C. D. (2011). Characterization of recycled aggregate concrete. *International Journal of Advanced Engineering Technology*, *2*(4), 321–330.

Tam, W. Y. V., Wang, Z. B., Tao, Z. B., & Tao, T. (2014). Behaviour of recycled aggregate concrete filled stainless steel stub columns. *Materials and Structures*, *47*, 293–310.

Xiao, J. Z., Huang, X., & Shen, L. M. (2012). Seismic behavior of semi-precast column with recycled aggregate concrete. *iConstructon and Building Materials*, *35*, 988–1001.

Xiao, J.Z, Li, W. G., Fan, Y. H., & Huang, X. (2012). An overview of study on recycled aggregate concrete in China (1996–2011). *Construction and Building Materials*, *31*, 364–383.

Xiao, J.Z., Pham, T. L., Wang, P. J., & Gao, G. (2014). Behaviors of semi-precast composite beams made with recycled aggregate concrete. *Structural Design of Tall and Special Buildings*, *23*, 692–712. http://doi.org/10.1002/tal.1071

Xiao, J., Pham, T. L., & Ding, T. (2015). Shake Table Test on Seismic Response of a Precast Frame with Recycled Aggregate Concrete. *Advances in Structural Engineering*, *18*(9), 1517–1534. http://doi.org/10.1260/1369-4332.18.9.1517

Xiao, J. Z., Sun, C., & Jiang, X. H. (2015). Flexural behaviour of recycled aggregate concrete graded slabs. *Structural Concrete*, *16*, 249–261.

Xiao, J. Z., Tawana, M. M., & Wang, P. J. (2010). Test on the seismic performance of frame joints with pre-cast recycled concrete beams and columns. In *The 2nd International Conference on Waste Engineering and Management*. Shanghai, China.

Xiao, J. Z., Wang, C. Q., Li, J., & Tawana, M. (2012). Shaking table model tests on recycled aggregate concrete frame structure. *ACI Structural Journal*, *109*, 777–786.

Zhang, M. (1997). Study on Similitude Laws for Shaking Table Tests. *Earthquake Engineering and Engineering Vibration*, *17*(2), 52–58.